PHYSICAL REVIEW B

CONDENSED MATTER AND MATERIALS PHYSICS

THIRD SERIES, VOLUME 61, NUMBER 11 **15 MARCH 2000-I**

BRIEF REPORTS

Brief Reports are accounts of completed research which, while meeting the usual **Physical Review B** *standards of scientific quality, do not warrant regular articles. A Brief Report may be no longer than four printed pages and must be accompanied by an abstract. The same publication schedule as for regular articles is followed, and page proofs are sent to authors.*

Ballistic-electron-emission microscopy of conduction-electron surface states

M. K. Weilmeier, W. H. Rippard, and R. A. Buhrman

School of Applied and Engineering Physics, Cornell University, Ithaca, New York 14853-2501

(Received 10 August 1999)

Cu/Au, Ag/Au, and Au/Cu/Au bilayer and trilayer (111) films grown on Si(111) and Si(100) substrates exhibit a spiral grain topography that, as determined by scanning tunneling spectroscopy, yields a high density of conduction-electron surface states on the flat areas of these grains. This results in strong spatial variations in the ballistic-electron-emission microscopy (BEEM) current due to differences in the proportion of electrons which tunnel into bulk as opposed to surface states. This enables BEEM imaging of variations in the density of unoccupied surface states and the examination of the effect of incomplete coverages of adatoms in coupling such surface states to the bulk.

In recent years the two-dimensional, conduction-electron surface states that form on the close-packed faces of the noble metals have received renewed and widespread attention [see, e.g. Refs. 1–13]. These surface states arise from the lack of propagating bulk states at and about the Fermi surface of these metals in a cone centered on the (111) direction. The interest in these states is due in part to the roles they can play in surface phenomena and thin-film growth,[2,3] but also because of the ability of the scanning tunneling microscope (STM) to locally image and study these states with high precision.[4–10] With the STM spectacular images have been obtained of confinement of surface states by ''quantum corrals'' of individually placed atoms,[6,8] and by the formation of small mesas or terraces on the surface of a properly oriented metal crystal.[7,9,10]

Here we present results from a different scan probe method used in the investigation of surface states on thin-film noble metal (111) surfaces; ballistic electron emission microscopy (BEEM).[14,15] In BEEM those energetic electrons are measured which are tunnel injected by an STM tip onto a metal surface, and hence travel, without undergoing inelastic scattering, to and through a buried Schottky barrier interface. Since surface states are strictly orthogonal to the bulk electronic states of a metal, at least in the ideal case of a clean and atomically flat metal (111) surface, electrons which tunnel into surface states will not contribute to the BEEM current. As we show below, this can provide a new means of directly imaging the spatial variation of unoccupied surface states on a thin film. It also provides a unique method for assessing the coupling generated between surface and bulk states by submonolayer coverages of adatoms.

The metal film samples in this study were grown in ultra-high-vacuum (UHV) on hydrogen-passivated Si(111) and Si(100) substrates and studied in an attached, room-temperature UHV/STM/BEEM system. In all cases a thin Au film, typically 10 nm thick, was first deposited onto these surfaces by thermal evaporation, forming a high quality Au-Si Schottky diode. X-ray measurements, which have been reported elsewhere,[16] show these Au films to be polycrystalline, but with the grains highly oriented such that their (111) crystal axes are normal to the substrate. All imaging was performed with etched polycrystalline tungsten tips having undergone *in situ* oxide removal and sharpening.[17]

Most of the samples discussed here are bilayer samples produced by depositing a second (Cu or Ag) thin-film overlayer, typically 3 to 10 nm thick, immediately following the initial deposition of the 10 nm Au (111) layer. X-ray 2-Θ diffraction measurements show that this overlayer is completely (111) oriented by the underlying Au, with its lattice constant being that expected for the bulk material and its in-plane alignment directly following that of the Au film. As illustrated in Fig. 1, STM measurements show that this deposition step results in the formation of a surface consisting of terraced grains characteristic of a spiral growth mechanism.[18] This spiral growth mode can be attributed to the preferential Cu (or Ag) atom deposition at the step edges of the Au film due to the lattice mismatch between Cu (Ag) and Au. Often the top mesa surface of the grain is transected by an atomic step, as indicated by arrows in Fig. 1, which we interpret as

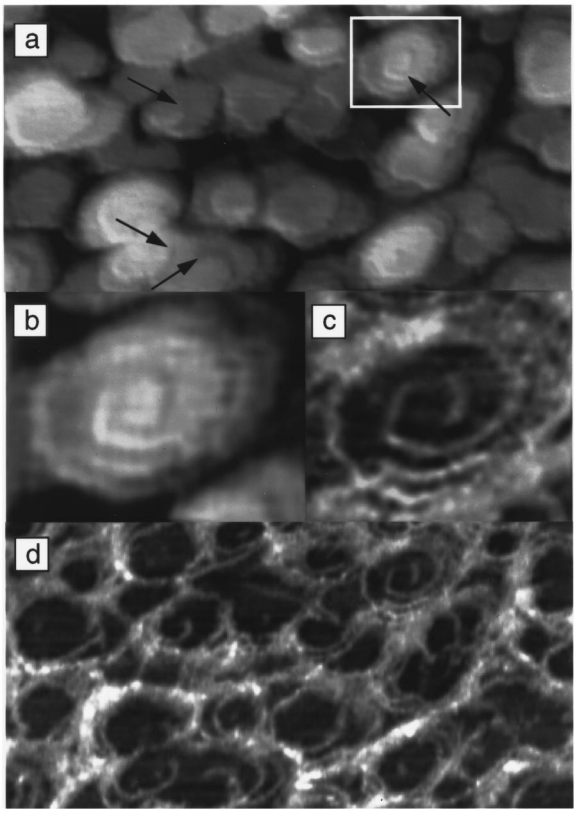

FIG. 1. STM surface topography and BEEM images of a Cu(2 nm)/Au(10 nm)/Si(111) sample obtained at $V_t=-1.1$ V and $I_t=1$ nA. (a) the STM surface height of a 100 nm×50 nm area of the Cu surface (2.5 nm white to black.) (b) an expanded image of the grain outlined in (a). (c) and (d) are the corresponding maps of the BEEM current I_c for (b) and (a) respectively. The mean current over the BEEM image is 7.3 pA, which has been subtracted from the image to enhance the contrast. The variation from white (high) to black (low) is 6 pA. The arrows indicate locations of terminating surface steps in the spiral grains.

the end of the screw dislocation that is the origin of the spiral form of the grain shown, e.g., in Fig. 1(b). Surrounding the grains, which are typically 10 nm or so in extent, or each small cluster of such grains, is an ~0.4 nm or deeper ''trench'' between it and its neighbors. For some samples, an additional Au overlayer 3–10 nm thick was subsequently deposited onto the Cu surface. This results in a Au surface with a topography very similar to that of the underlying Cu surface. All depositions were done in a pressure of $<2\times10^{-10}$ Torr.

STM current-voltage (I-V) measurements taken at various locations on the mesas and terraces of the samples invariably indicated the presence of the two-dimensional conduction-electron surface states, as seen previously in STM experiments on bulk single-crystal and epitaxial thin-film Cu, Ag and Au (111) surfaces.[2–10] The noble-metal surface states have been measured by photoemission to have their band minima at 0.41, 0.39, and 0.12 eV below the Fermi level, for Au, Cu, and Ag, respectively.[1] In Fig. 2 we show dI/dV vs V measurements, which are roughly proportional to the local density of states on the surface of the metal,[6–9] as made near the center of >10 nm diameter mesas of a Au/Cu/Au/Si sample and a Cu/Au/Si sample, and at the center of an ~3 nm diameter mesa on a Ag/Au/Si sample.

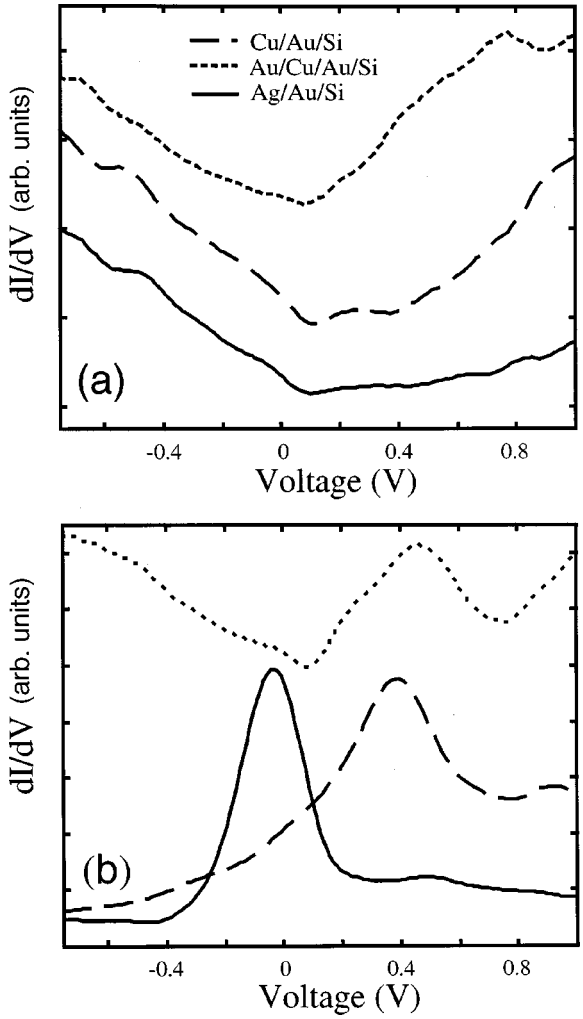

FIG. 2. (a) dI/dV spectra taken with the STM tip above grain boundaries on the surface of Au/Cu/Au/Si, Cu/Au/Si, and Ag/Au/Si samples. (b) dI/dV spectra taken above the center of mesas on the same surfaces. The spectra are obtained by averaging 100 I-V's taken at the same location. In the case of the Au and Cu surfaces the mesa diameter was ~10 nm, for Ag ~3 nm.

There are strong, albeit thermally rounded, peaks in dI/dV, indicative of the onset of tunneling from the surface states as the tip bias sweeps through the minimum of their respective conduction bands. For the Au surface the peak is at ~+0.45 V (referenced to the tip bias), for Cu the peak is at ~+0.4 V, and at approximately 0 V for Ag. The shifted Ag result is due to quantum confinement effects on this comparatively small mesa.[10] In accord with previous studies we also found that dI/dV measurements made at step edges and grain boundaries, also illustrated in Fig. 2, showed only a very small surface state signal or none at all, particularly in the latter case. Thus we conclude that the spiral-grain, terraced topography of these Cu/Au, Ag/Au, and Au/Cu/Au thin-film multilayers is very favorable for the formation of surface states on these terraces.

In BEEM imaging, the STM tip is scanned across a sample surface while maintaining a constant tunneling current I_t, generally 1–2 nA, and with a fixed tip bias which is set −1.0 to −1.3 V in our experiments, above the Schottky barrier height of the interface. Figure 1(c) is a map of the BEEM current I_c obtained while also obtaining the topographical image of Fig. 1(b), while Fig. 1(d) is the BEEM

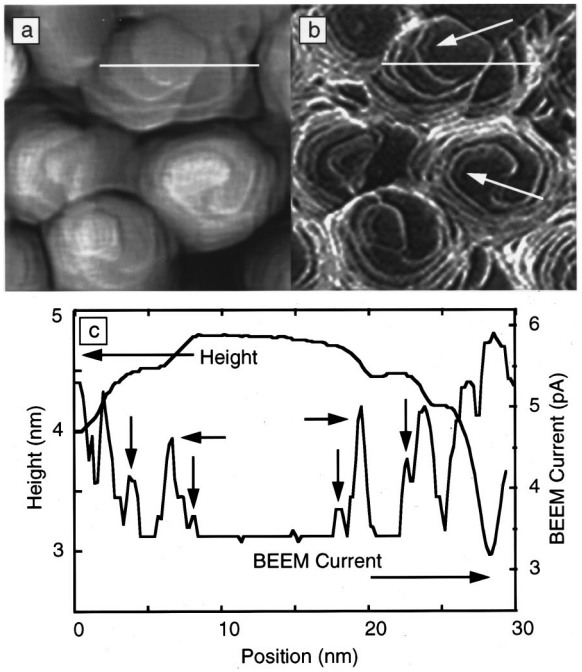

FIG. 3. (a) STM surface topography (3.5 nm white to black), and (b) BEEM image of a Au(10 nm)/Cu(3.5 nm)/Au(10 nm)/Si(100) sample. Images are 50 nm×50 nm and are obtained at $V_t = -1.0$ V and $I_t = 1.5$ nA. The mean current over the BEEM image is 4.8 pA, which has been subtracted from the image to enhance the contrast. The variation from white (high) to black (low) is 4.1 pA. The arrows in (b) indicate locations of BEEM ''echoes.'' (c) shows line scans taken across the region of sample indicated by the horizontal white lines in (b). The horizontal arrows indicate locations of enhanced I_c at surface steps, the vertical arrows locations of enhanced I_c from minima in the surface state standing wave.

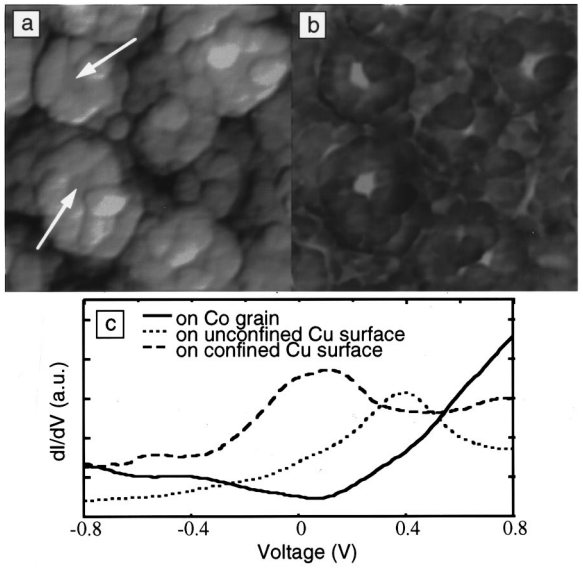

FIG. 4. (a) STM surface topography (2.5 nm white to black), and (b) BEEM image of a 50 nm×50 nm Co(0.30 nm)/Cu(3 nm)/Au(10 nm)/Si(111) sample. $V_t = -1.1$ V and $I_t = 2.0$ nA. The mean current over the BEEM image is 4.7 pA and the variation from white (high) to black (low) is 7 pA. The Co layer does not fully cover the surface, leaving small enclosed areas of Cu mesas exposed, such as indicated by the arrows in (a). Due to the strong BEEM attenuation of the Co layer the Cu surfaces are now relatively ''bright'' in the BEEM image. (c) dI/dV spectra as taken with the STM tip above an enclosed Cu surface, which shows the surface state signal, shifted due to quantum confinement by the encroaching Co; above a Co coated region; and above a different Cu surface with no Co deposit.

image of the Cu/Au/Si(111) surface shown in Fig. 1(a). There are very strong BEEM variations in the image, with I_c varying by nearly a factor of 2. With one exception discussed below, the regions of high BEEM current are completely correlated with regions where the surface topography changes rapidly, i.e., at steps and grain boundaries.

In Fig. 3 we show the topographical image for a Au/Cu/Au/Si(100) sample, together with the simultaneously obtained BEEM image. Again the BEEM image shows very strong variations in I_c as the tip scans from the mesa top of a grain, across the spiral steps and across its surrounding grain boundary. We note that similar results are obtained with Ag/Au bilayer samples, and, as illustrated by Figs. 1 and 3, the choice of a Si(100) or Si(111) substrate has no substantial effect on this BEEM behavior. Extensive investigation has also ruled out standard scan probe experimental artifacts as the explanation for this contrast.

We conclude that this strong BEEM contrast is the direct consequence of the band structure of these (111) oriented UHV-grown films, and the resultant formation of a high density of surface states on the flat areas of their surfaces. When the tip is positioned above a flat area, as much as half of the tunnel current is injected into the surface states as compared to when the tip is above a step or grain boundary. The enhanced I_c at steps and grain boundaries is then due to the reduced density of surface states at these locations. For those electrons that tunnel into bulk states, the metal band structure acts to channel their paths into favorable off-normal directions as they proprogate further into the metal film.[19] This facilitates the interface transmission for both the Si(111) and Si(100) substrates, and thus explains the similarity of the results for the two Si orientations.[16]

BEEM contrast correlated with surface structure has been previously observed, but typically of smaller amplitude.[15] In the case of epitaxial silicide layers on Si(111) substrates, this contrast is due to surface structure or defects imparting transverse momentum to the ballistic electrons, which can enhance the interface transmission due to the conduction band offset of Si(111).[20] With polycrystalline metal films on GaP(110) substrates the BEEM current was *attenuated* at grain boundaries, which was attributed to elastic scattering *decreasing* the transmission rate into that conduction-band-centered substrate.[21] In those cases the metal band structure did not forbid electron transport normal to the substrate and thus there was no involvement of surface states. Finally, we note that BEEM contrast effects have generally not been seen previously for Au on Si, possibly due to the morphology or orientation of the Au grains in those studies.[22]

Figure 3(b) reveals an additional effect which is seen on some samples and which serves to confirm the surface state explanation for the contrast. There inside the ring of high I_c that surrounds each flat region, a weaker ''echo'' ring is generally present. The arrows in Fig. 3(b) point out two examples of this. As illustrated by the topographical and BEEM line scans shown in Fig. 3(c), these echo rings of enhanced I_c are not correlated with surface structure at their location. Their presence is consistent with the existence of a

standing wave pattern in the local density of surface states due to the reflection of surface electrons from the repulsive barrier that arises at the mesa edge.[6–9] This reflection results in the surface state density r_s varying as $r_s(E,x) \sim 1 - J_0(2kx)$ where J_0 is the first-order Bessel function, k the surface electron wave vector and x the distance from the potential barrier.[6,7] The second minimum in r_s should then occur at $2kx=7$, or $x \approx 1$ nm since the wavelength of the Au surface state at 1.1 eV above the Fermi energy is approximately 1.8 nm, using photoemission results for the effective mass of the surface electrons.[1] This is in accord with the ~ 1 nm separation between the onset of the high BEEM current at the edge of the mesas and the position of the peak of the BEEM echoes. We also note that these BEEM echoes are not observed next to positions where the surface exhibits a step-up. This is explained by the weaker potential barrier which the surface electrons see at the bottom of a step.[7] While there should also be a small change in the tip height corresponding to each of the changes in surface state density, our room temperature instrument lacks the resolution to observe these in the topographical image. We also point out that the off-axis lighting used in Fig. 3(b) to highlight the ''echoes'' tends to obscure those parts of these structures lying just to the left of a step-down in the image. However, such ''echoes'' are indeed present on the right-hand sides of the grains as is explicitly pointed out in Fig. 3(c) by the vertical arrows. Finally, these features are observed with equal intensity in both forward and reverse scan directions and so cannot be due to current overshoot induced by the feedback loop.

In pioneering quantum confinement studies it was concluded by Heller *et al.* that Fe impurity atoms when placed in a ring on the (111) surface of the noble metals to form quantum corrals were ''black dots'' in that the Fe atoms reflected only 25% of the incident surface electron wave, transmitted 25% and scattered the remaining 50% of the wave into bulk states.[8] This analysis utilized measurements of the spatial and energy dependence of the local density of states of a confined two-dimensional electron gas system. Crampin and co-workers have also examined this confinement problem and find with their model that scattering into bulk states is much more important than tunneling through the corral walls in determining the widths of the confined levels.[11,12] Harbury and Porod on the other hand have concluded that tunneling through the confinement wall into other surface states is the dominant line-broadening process.[13]

To further test our surface state explanation for the BEEM contrast, and to examine the effect of impurity adatoms on normally unoccupied surface states, we have deposited submonolayer and monolayer level coverages of Co atoms onto Cu/Au/Si samples. Images from one such sample are shown in Fig. 4. We find that the Co atoms first adhere preferentially to the top edges of the Cu steps and grain boundaries, forming incomplete rings of Co atoms around the spiral grain mesas. As more Co is deposited, these rings become complete, and then the Co grows inward to form a continuous coverage at a mean Co thickness of ~ 0.4 nm. Until the coverage is complete the Co covered areas can be distinguished from the Cu mesas in part by their different topography, as illustrated in Figs. 1(a) and 4(a). The identity of the surface species is further confirmed by dI/dV measurements which show surface states on the mesas, indicating that they are Cu, but which show a lack of such states on the rings around the mesas, indicating they are Co surfaces which do not support surface states. Of course as the exposed Cu mesas grow smaller, the energy of the conduction band minima of the Cu surface state band shifts upwards due to quantum confinement, as illustrated in Fig. 4(c).

The strength of the BEEM signal when the STM tunnels to the uncovered Cu is unchanged by the presence of the surrounding Co, to $\sim 10\%$ accuracy, while I_c for areas covered by Co is substantially attenuated, presumably due to the band-structure mismatch between Co and Cu. The lack of any significant increase in I_c from the Co confinement leads us to conclude that the rings of Co atoms do not substantially increase the elastic coupling of these surface states into Cu bulk states that can propagate to the Si interface. We also note that the lack of enhanced BEEM current at the Co-covered steps and grain boundaries is fully consistent with the contrast, illustrated in Figs. 1 and 3, being due to tunneling to a spatially varying density of surface states, and not simply to a tunneling geometry effect.

This research was supported in part by the Office of Naval Research and by the Air Force Office of Scientific Research. Support was also provided by NSF through use of the facilities of the Cornell Center for Materials Research and through use of the National Nanofabrication Users Network.

[1] D. Kevan and R. H. Gaylord, Phys. Rev. B **36**, 5809 (1987).
[2] N. Memmel and E. Bertel, Phys. Rev. Lett. **75**, 485 (1995).
[3] E. Bertel, Phys. Status Solidi A **159**, 235 (1997).
[4] W. J. Kaiser and R. C. Jaklevic, IBM J. Res. Dev. **30**, 411 (1986).
[5] L. C. Davis, M. P. Everson, R. C. Jaklevic, and Weidian Shen, Phys. Rev. B **43**, 3821 (1991).
[6] M. F. Crommie, C. P. Lutz, and D. M. Eigler, Science **262**, 524 (1993).
[7] Y. Hasegawa and Ph. Avouris, Phys. Rev. Lett. **71**, 1071 (1993).
[8] E. J. Heller, M. R. Crommie, C. P. Lutz, and D. M. Eigler, Nature (London) **369**, 464 (1994).
[9] Ph. Avouris, I.-W. Lyo, and P. Molinas-Mata, Chem. Phys. Lett. **240**, 423 (1995).
[10] J. T. Li, W. D. Schneider, R. Berndt, and S. Crampin, Phys. Rev. Lett. **80**, 3332 (1998).
[11] S. Crampin, M. H. Boon, and J. E. Inglesfield, Phys. Rev. Lett. **73**, 1015 (1994).
[12] S. Crampin and O. R. Bryant, Phys. Rev. B **54**, R17 367 (1996).
[13] H. H. Harbury and W. Porod, Phys. Rev. B **53**, 15 455 (1996).
[14] W. J. Kaiser and L. D. Bell, Phys. Rev. Lett. **60**, 1406 (1988).
[15] M. Prietsch, Phys. Rep. **253**, 163 (1995).
[16] M. K. Weilmeier, W. H. Rippard, and R. A. Buhrman, Phys. Rev. B **59**, R2521 (1998).
[17] O. Albrektsen *et al.*, J. Vac. Sci. Technol. B **12**, 3187 (1994).
[18] W. K. Burton, N. Cabrera, and F. C. Frank, Philos. Trans. R. Soc. London, Ser. A **243**, 299 (1951).
[19] F. J. Garcia-Vidal, P. L. de Andres, and F. Flores, Phys. Rev. Lett. **76**, 807 (1996).
[20] H. Sirringhaus, E. Y. Lee, and H. von Kanel, Phys. Rev. Lett. **73**, 577 (1994).
[21] M. Prietsch and R. Ludeke, Phys. Rev. Lett. **66**, 2511 (1991).
[22] E. Y. Lee *et al.*, J. Vac. Sci. Technol. B **11**, 1579 (1993).